0026-895X/97/061087-08$3.00/0

MOLECULAR PHARMACOLOGY, **52:**1087–1094 (1997).

Site-Directed Mutagenesis on the m2 Muscarinic Acetylcholine Receptor: The Significance of Tyr403 in the Binding of Agonists and Functional Coupling

WALTER K. VOGEL, DAVID M. SHEEHAN, and MICHAEL I. SCHIMERLIK

Department of Biochemistry and Biophysics (W.K.V., D.M.S., M.I.S.) and Environmental Health Sciences Center (M.I.S.), Oregon State University, Corvallis, Oregon 97331-7305

Received April 21, 1997; Accepted August 18, 1997

SUMMARY

The first step in the transmembrane signal mediated by G protein-coupled receptors is binding of agonist to receptors at the cell surface. The mechanism of the resulting receptor activation is not clear, but models based on the ternary complex model are capable of explaining most of the observations that have been reported in G protein-coupled receptors. This model suggests that a single agonist/receptor/G protein complex capable of activating G protein is formed as the result of agonist binding. Extensions of this basic model differ primarily in whether an equilibrium between active and inactive conformations is required to explain experimental results. We report results on ligand binding and coupling to physiological effector systems of the m2 muscarinic acetylcholine receptor site-directed mutant Y403F (residue 403 mutated from tyrosine to phenylalanine) expressed in Chinese hamster ovary cells and compare our results with results reported for the homologous Y506F mutation in the m3 muscarinic receptor [*J. Biol. Chem.* **267:**19313–19319 (1992)]. The mutation in the m2 muscarinic receptor reduced absolute agonist affinities more dramatically than in the m3 muscarinic receptor. Unlike the results reported for the m3 subtype mutant, in which coupling to physiological effector systems was reduced, coupling to effector systems for the mutant in the m2 subtype was robust. In the Y403F m2 muscarinic receptor, the difference between the two agonist binding affinities was greater than in the wild-type receptor, whereas in the m3 subtype, the effect of the mutation was to decrease this difference. A prediction of the ternary complex model is that relative binding affinities will affect the steady state concentration of the agonist/receptor/G protein complex and, as the result, the extent of G protein coupling. These results can best be rationalized by this model, which suggests that the activation of G protein-coupled receptors is achieved by the relative affinity of agonist for two receptor states and does not require the existence of multiple states in conformational equilibrium.

Muscarinic acetylcholine receptors are members of a diverse group of receptors and sensory proteins that are characterized structurally by a pattern of hydrophobic residues suggesting seven transmembrane domains and functionally by coupling the binding of an extracellular activator to intercellular effector via G proteins. Five muscarinic receptor subtypes (m1–m5) have been cloned and expressed (1–5). The odd-numbered subtypes couple preferentially to the stimulation of phospholipid metabolism, and the even-numbered subtypes couple preferentially to the inhibition of cAMP formation. The m2 subtype is widely distributed in mammalian tissue and is the only subtype found in mammalian heart (3), where it acts via the cardiac pacemaker cells to activate inwardly rectifying potassium channels in addition to inhibiting adenylyl cyclase and stimulating phospholipid metabolism (6). Two results of agonist binding to the cardiac m2 muscarinic receptor are a decrease in heart rate, due to the activation of inwardly rectifying potassium channels, and a decrease in the force of contraction, due to the reduction in voltage-gated calcium currents regulated indirectly via cAMP levels (7).

The agonist binding site of G protein-coupled receptors is thought to lie in the transmembrane bundle of amphipathic α-helices. Photochemical cross-linking with an analog of 11-*cis*-retinal predominantly labeled the third and sixth transmembrane helices, suggesting that they make up part of the retinal binding site of rhodopsin (8). Among G protein-coupled receptors that bind biogenic amines, a conserved aspartate residue in the third transmembrane helix is critical for the binding of ligand (9–11). We report results from the site-directed mutant Y403F (residue 403 mutated from tyrosine to phenylalanine) in the m2 muscarinic receptor,

This work was supported by National Institutes of Health Grants HL23632 and ES00210.

ABBREVIATIONS: CHO, Chinese hamster ovary; NMS, *S*-(−)-*N*-methylscopolamine; QNB, *R*-(−)-quinuclidinyl benzilate; EGTA, ethylene glycol bis(β-aminoethyl ether)-*N*,*N*,*N*′,*N*′-tetraacetic acid; HEPES, 4-(2-hydroxyethyl)-1-piperazineethanesulfonic acid.

which is located in the sixth transmembrane helix one residue beyond a highly conserved proline. Results from studies in the β-adrenergic (12) and bradykinin (13) receptors in which the homologous residue is a phenylalanine and from studies in the m3 muscarinic receptor (14, 15), rhodopsin (16), and the neurokinin-2 receptor (17) in which the homologous residue is a tyrosine suggest that these residues are part of or near the agonist/retinal binding sites of these G protein-coupled receptors.

The nature of the relationship between agonist binding to G protein-coupled receptors and the activation of G proteins is poorly understood. Models of G protein activation differ in the number of states of the receptor. The simplest models rely on two receptor states with respect to agonist and G protein binding (scheme given in Fig. 1). Agonist binds free receptor and G protein-complexed receptor that have different agonist affinities, and G protein binds free receptor and agonist-complexed receptor that have different G protein affinities. This ternary complex model results in two G protein-complexed states: the receptor/G protein binary complex and the agonist/receptor/G protein ternary complex. G protein activation occurs via the ternary complex (18, 19) or via both the binary and the ternary complexes at different rates (20). The basic model was extended to explain a constitutively active β-adrenergic receptor mutant (21), negative antagonism (22), and inverse agonist activity (23), and these extensions have been generalized into the cubic ternary complex model in which each state represented in the scheme in Fig. 1 is proposed to exist in an active and inactive conformation. These models describe G protein-coupled receptors as existing in multiple states of activity in which agonists promote the more active state and inverse agonists promote the less active state by mass action. The simpler model suggests that agonists activate G protein-coupled receptors by occupancy. The binding of agonist to the two linked states of the receptor results in greater concentrations of the agonist/receptor/G protein complex as the ratio of agonist affinities increases and is a measure of intrinsic efficacy of an agonist in a given receptor/G protein system (19). Here, efficacy is defined as the ability of an agonist to promote a physiological response independent of the absolute affinity of the agonist for the receptor.

The difference between the above models is whether receptor occupancy, and therefore the maintenance of a steady state concentration of agonist/receptor/G protein complex, is the primary mode of receptor activation. The alternative is that a conformational equilibrium between active and inactive receptor states plays the primary role and receptor occupancy plays a secondary role. The choice of model has a practical consideration in the drug design process in the attention paid to agonist-receptor binding characteristics.

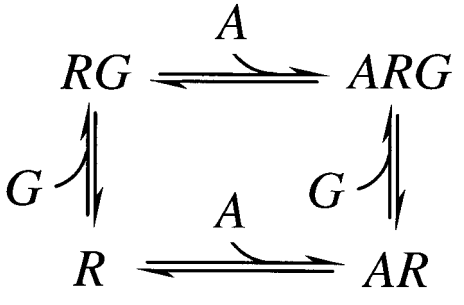

Fig. 1. Ternary complex model describing the binding of agonist and G protein to G protein-coupled receptors. *A*, agonist; *G*, G protein; *R*, free receptor; *AR*, agonist-bound receptor; *RG*, G protein-bound receptor; *ARG*, agonist/G protein/receptor ternary complex.

The m2 muscarinic receptor expressed at high levels in CHO cells is a system especially well suited for the evaluation of models of G protein-coupled receptors because the agonist affinities are well separated and clearly defined in competition binding assays. A relationship between the ratio of agonist affinities in muscarinic receptors and apparent efficacy was first reported by Birdsall *et al.* (24). Our results identify a specific tyrosine residue that is important for agonist binding in the m2 muscarinic receptor. Similar but less dramatic effects on agonist binding were reported for the homologous mutation in the m3 muscarinic receptor (14, 15). Unlike the results in the m3 subtype, in which mutation of this tyrosine resulted in diminished coupling to effector systems, this mutation in the m2 subtype resulted in increased coupling. The effects of these mutations correlate with changes in the ratio of agonist affinities for *RG* compared with *R* (scheme in Fig. 1) that increase in the m2 subtype but decrease in the m3 subtype. The correlation of decreased agonist affinity with decreased coupling to an effector system led Wess *et al.* (15) to conclude that this tyrosine is part of a binding and trigger mechanism in the m3 subtype serving in both agonist binding and activation of G proteins. We argue against this explanation of the results for the m3 mutation and suggest that the ternary complex model provides an adequate explanation of the results from both subtypes.

Experimental Procedures

The procedures used to produce stably transfected clonal CHO cell lines overexpressing wild-type and mutant receptor (2) and enriched membrane preparations (25, 26) were described previously.

Materials. [^{3}H]QNB, [^{3}H]NMS, and [^{14}C]cAMP were purchased from DuPont New England Nuclear Research Products (Boston, MA). [^{3}H]Adenine and *myo*-[^{3}H]inositol were from American Radiolabeled Chemicals (St. Louis, MO). Acetylcholine was from Sigma Chemical (St. Louis, MO). Carbachol and pilocarpine were from Aldrich Chemical (Milwaukee, WI). Oxotremorine M was from Research Biochemicals (Natick, MA). Ro 20–1724 was from BIOMOL Research Laboratories (Plymouth Meeting, PA). Guanylyl-imidodiphosphate was from Boehringer-Mannheim Biochemicals (Indianapolis, IN).

Site-Directed Mutagenesis. The Y403F mutant porcine m2 muscarinic receptor was produced by oligonucleotide-directed mutagenesis according to the method of Vandeyar *et al.* (27) except that *Escherichia coli* ER1451 was used. The mutation was introduced by priming second strand synthesis with the antisense oligonucleotide: 5′-ATGACGTTGAACGGGGCCCAA-3′ (the base change is underlined). The wild-type coding region was ligated into M13mp18 as a *Hin*dIII/*Eco*RI fragment derived from the pSVE expression vector (2) kindly provided by Dr. Daniel Capon (Genentech, South San Francisco, CA). The sequence of the Y403F was confirmed by dideoxy sequencing (28). The mutated coding region was ligated into the pSVE expression vector and used to transfect CHO cells.

Effector Coupling. Phosphatidylinositol stimulation was determined in attached CHO cells expressing Y403F muscarinic receptor plated at 2×10^4 cells/mm^2 and incubated in 4 μCi/ml *myo*-[^{3}H]-inositol for 72 hr. Agonists were added, and inositol 1-phosphate accumulation was measured after 30 min at 37° as described by Lee *et al.* (29). Inhibition of forskolin-stimulated adenylyl cyclase activity was determined in attached confluent CHO cells in the presence of 100 μM isobutylmethylxanthine, 50 μM Ro 20–1724, and agonist

after exposure of the cells to 8 μCi/ml [^{3}H]adenine for 2–3 hr. The 20-min assay at 37° was started by the addition of 40 μM forskolin, and [^{3}H]cAMP was determined according to the method of Salomon (30). Results for Y403F mutant and wild-type were compared at similar levels of expression in cloned cells lines.

Ligand Binding. Ligand binding to enriched membrane preparations was assessed in 10 mM HEPES, 5 mM $MgCl_2$, 1 mM EDTA, and 1 mM EGTA, pH 7.4 at 25°. After 4–6 hr, samples were filtered through Schleicher & Schuell (Keene, NH) No. 32 glass-fiber filter membranes pretreated with 0.1% (w/v) polyethylenimine on a Brandel Harvester (Gaithersburg, MD) and washed with ~10 ml of ice-cold 50 mM sodium phosphate and 1 mM EDTA, pH 7.4. Nonspecific binding was assessed in the presence of 1–4 × 10^4-fold excess unlabeled ligand. In direct binding experiments on the Y403F mutant, the receptor site concentrations were 140–350 pM ([^{3}H]NMS) and 60–110 pM ([^{3}H]QNB). In competition binding experiments with [^{3}H]NMS (2.5–6.5 nM), the receptor site concentration was 60–390 pM.

Protein Stability. Resistance to thermal inactivation was assessed in enriched membrane preparations in the presence and absence of saturating [^{3}H]QNB. Membranes were exposed to different temperatures for 1 hr and quenched on ice, and residual [^{3}H]QNB binding was determined.

Data Analysis. Functional assays were fit to eq. 1, where max_1 and max_2 are the maxima of the inhibitory and stimulatory portions of the curve, min is the minimum of the curve, $[x]$ is the agonist concentration, and $p1$ and $p2$ are the respective slope factors. For adenylyl cyclase assays that showed only an inhibitory phase, the first two terms were used, and for assays of phosphatidylinositol metabolism stimulation, the first and last terms were used.

$$\mathrm{CPM} = min + \frac{max_1 - min}{1 + \left(\frac{[x]}{(\mathrm{EC}_{50}i)}\right)^{p1}} + \frac{max_2 - min}{1 + \left(\frac{(\mathrm{EC}_{50}s)}{[x]}\right)^{p2}} \quad (1)$$

In direct saturation binding experiments, total bound radioligand was analyzed as the sum of specifically, $[RL]$, and nonspecifically, $N[L]$, bound ligand according to the quadratic solution of eqs. 2 and 3, where $[R_0]$ and $[L_0]$ are the total receptor and ligand concentrations, respectively; K is the equilibrium dissociation constant; and N is the proportionality constant of nonspecifically bound ligand to free ligand concentration.

$$[RL] = \frac{([R_0] - [RL])([L_0] - [RL])}{K(N+1)} \quad (2)$$

$$N[L] = \frac{N([L_0] - [RL])}{N+1} \quad (3)$$

Agonist binding was assessed in competition with radiolabeled antagonist. Agonist binding data were fit to two or three noninteracting classes of sites that bound antagonist with the same dissociation constant. Total labeled antagonist specifically bound, $[RL]$, is the sum of that bound at each subclass of agonist binding sites according to the polynomial solutions of eq. 4, as follows:

$$[RL] = \sum_{i=1}^{n} \frac{F_i[R_0]([L_0] - [RL])}{K(N+1)\left(1 + \frac{[\mathrm{A}]}{K_i}\right) + [L_0] - [RL]} \quad (4)$$

where $[R_0]$ is the total concentration of receptor, F_i is the fraction of $[R_0]$ in site i, $[L_0]$ is the total labeled antagonist concentration, [A] is the total agonist concentration (equal to the free concentration because no displacement occurs until [A] > $[R_0]$, K is the dissociation constant for radiolabeled antagonist, and K_i the dissociation constant for the agonist at site i (referred to as K_H, K_M, and K_L, the high, medium, and low affinity equilibrium dissociation constants, respectively). Data were fit by nonlinear least-squares procedures using Marquardt's algorithm (31), and parameter values are reported as the mean and 95% confidence interval of several determinations.

Ligand binding energetics. The difference in ligand binding energy between Y403F mutant and wild-type muscarinic receptor was calculated with eq. 5, as follows:

$$\Delta(\Delta G^\circ) = \Delta G^\circ_{\mathrm{Mutant}} - \Delta G^\circ_{\mathrm{Wild\text{-}type}} = RT \ln(K_{\mathrm{Mutant}}/K_{\mathrm{Wild\text{-}type}}) \quad (5)$$

where ΔG° is the standard Gibbs free-energy change, R is the gas constant, T is the absolute temperature, and K is the equilibrium dissociation constant. $\Delta(\Delta G^\circ)$ is the apparent binding energy contributed by the tyrosine hydroxyl (32); it does not take into account the changes in solvation of the mutant receptor or potential changes in receptor stability. $\Delta(\Delta G^\circ)$ is defined such that positive values indicate that the mutant binds ligand less strongly.

Results

Ligand binding properties of Y403F m2 muscarinic receptor were assessed in sucrose gradient enriched membrane preparations. Antagonists [^{3}H]NMS and [^{3}H]QNB bound to a single class of sites with affinities that were 2.5- and 1.7-fold lower than those for wild-type receptor, respectively. Agonists seemed to bind to two classes of sites compared with three for wild-type, with affinities (K_M values) that were 200–300-fold lower for acetylcholine and carbachol than for wild-type. The binding affinities for the agonists oxotremorine M and pilocarpine were less dramatically affected, being reduced by <100-fold (Table 1). Competition binding assays were conducted in the presence and absence of guanylylimidodiphosphate, a nonhydrolyzable analog of GTP; results for carbachol are shown in Fig. 2. Data in the presence and absence of guanine nucleotide were fit so that values for K_H and K_M were shared in the analysis of a given experiment (20). The highest affinity site, K_H, was sensitive to the presence of guanine nucleotide, which is consistent with binding to the G protein/receptor complex.

Among G protein-coupled receptors, agonists can be characterized by their affinity for free receptor and their ability to promote the formation of the agonist/receptor/G protein ternary complex over the agonist/receptor binary complex. Agonist affinity for free receptor is quantified by K_M values, whereas the ability to promote the ternary complex is described by the parameter α (19, 20), which is calculated as the quotient of K_M and K_H values (Table 1). The α values for Y403F were ~4, ~2, ~3, and ~0.6 times greater than those for wild-type receptor for acetylcholine, carbachol, oxotremorine M, and pilocarpine, respectively.

When comparing a mutant and wild-type protein, it is difficult to attribute differences in ligand affinity to a specific interaction between the mutated residue and ligand if the mutation also results in altered protein structure. Resistance to irreversible thermal inactivation in the presence and absence of the antagonist QNB was used to assess the effects of the mutation on m2 muscarinic receptor structure. Y403F was indistinguishable from wild-type receptor in its resistance to thermal inactivation, suggesting that loss of the tyrosine hydroxyl did not significantly destabilize receptor structure (Fig. 3).

Functional coupling of the mutant receptor was assessed in attached tissue culture cells, and the results were compared with data for wild-type receptor at similar expression levels (20). Acetylcholine, carbachol, and oxotremorine M stimulated phosphatidylinositol metabolism to a slightly greater

TABLE 1

Ligand binding properties of Y403F mutant and wild-type m2 muscarinic receptor

	K							Δ(ΔG°) (kcal · mol^{-1})	
	Y403F			Wild-type				*K*^{b}	
Antagonist									
[^{3}H]NMS		630 ± 240 (5)			253 ± 45 (15)			0.54 ± 0.22	
[^{3}H]QNB		29.3 ± 3.4 (3)			17.4 ± 2.8 (16)			0.31 ± 0.10	
	K_H	K_M	α^a	K_H	K_M	K_L	α^a	K_H^b	K_M^b
	nM	μM		nM	μM	μM			
Agonist									
Acetylcholine	107 ± 51 (3)	101 ± 36 (4)	950 ± 560	1.45 ± 0.49 (12)	0.350 ± 0.087 (15)	11.1 ± 3.9 (13)	240 ± 100	2.55 ± 0.25	3.36 ± 0.21
Carbachol	390 ± 170 (5)	248 ± 68 (5)	630 ± 320	3.6 ± 0.80 (19)	1.37 ± 0.16 (38)	21.7 ± 3.7 (37)	380 ± 100	2.77 ± 0.26	3.08 ± 0.16
Oxotremorine M	51 ± 43 (5)	25.8 ± 4.5 (5)	500 ± 430	2.16 ± 0.89 (10)	0.40 ± 0.14 (16)	13.0 ± 8.2 (9)	190 ± 100	1.88 ± 0.49	2.47 ± 0.22
Pilocarpine	2370 ± 680 (6)	149 ± 52 (7)	63 ± 29	27 ± 17 (8)	2.78 ± 0.73 (14)	25 ± 16 (9)	100 ± 70	2.65 ± 0.39	2.36 ± 0.24

Values are the weighted mean ± 95% confidence interval; the number of experimental determinations are indicated in parentheses.
Δ(ΔG°) values are presented ± 95% confidence interval.
[a] α is calculated as the quotient of the parameters K_M and K_H.
[b] Equilibrium constant for which the Δ(ΔG°) values are calculated.

Fig. 2. [^{3}H]NMS displacement by carbachol in Y403F CHO cell membranes. Data were fit to two independent classes of sites, as described in Experimental Procedures. The parameter values for the fitted lines are shown ± asymptotic standard errors. K_H = 0.64 ± 0.14 μM, K_M = 238 ± 9 μM, and F_H = 39.9 ± 1.4% in the absence of guanylyl-imidodiphosphate (●) and 13.6 ± 2.0% in the presence of 200 μM guanylyl-imidodiphosphate (○). *Inset,* [^{3}H]NMS binding to the same membrane preparation presented as a Scatchard plot (33) (K = 813 ± 29 pM). The concentration of [^{3}H]NMS for the carbachol competition was 5.7 nM, and the receptor site concentration for both the competition and direct binding of [^{3}H]NMS was 190 pM.

Fig. 3. Irreversible thermal inactivation of Y403F m2 muscarinic receptor. Experiments were done in the absence (○, □, △) and presence (●, ■, ▲) of saturating antagonist [^{3}H]QNB. The $T_{0.5}$ values were 51.8 ± 1.0° (three experiments) in the absence and 59.1 ± 1.8° (three experiments) in the presence of saturating QNB. *Horizontal bars*, mean and 95% confidence interval of results from wild-type receptor, 54.1 ± 1.6° (15 experiments) in the absence and 60.2 ± 1.3° (16 experiments) in the presence of saturating QNB. These differences were not significantly less than wild-type (p = 0.05). QNB stabilized the receptor by 7.3 ± 1.3° in a paired sample analysis, a value not significantly different from wild-type (6.2 ± 0.9°).

extent than wild-type, whereas the EC_{50} values were greater than wild-type by 150, 120, and 40, respectively (Table 2). These increases in EC_{50} values are similar to the increase in K_M values: 290, 180, and 65 for acetylcholine, carbachol, and oxotremorine M, respectively (Table 1). The values of K_M and the EC_{50} for stimulation of phosphatidylinositol metabolism were found to be approximately equal for the wild-type receptor, and this was rationalized as coupling via a G protein that has a relatively low affinity for the receptor (20). The mutant receptor seemed to stimulate phosphatidylinositol metabolism to a greater extent than wild-type with acetyl-

TABLE 2

Effect of Y403F mutation on phosphatidylinositol stimulation in whole-cell assays

Values for EC_{50} and fold maximal stimulation of phosphatidylinositol metabolism are shown for the indicated receptor site densities. These values are compared with the wild-type values for the same range of receptor site densities observed in wild-type-expressing CHO cells from data previously reported (20). Results with pilocarpine were not significant. EC_{50} values are presented ± standard deviation.

Agonist	*n*	EC_{50}	Stimulation[a]	[R]	Wild-type EC_{50}	Wild-type stimulation
		μM	*fold*	*pmol · dm*$^{-2}$	*μM*	*fold*
Acetylcholine	2	60 ± 4	1.6–2.6	1.3–5.0	0.4 ± 0.2	1.2–1.4
Carbachol	4	140 ± 70	2.4–3.0	5.0–33	1.2 ± 0.5	1.6–2.4
Oxotremorine M	2	40 ± 3	1.6–2.6	1.3–5.0	1.0 ± 0.5	1.4–1.5
Pilocarpine	6	N.S.	N.S.	0.7–10.8	10 ± 4	1.1–1.3

[a] Maximal stimulation increased with increasing [R] as in wild-type.

choline, carbachol, and oxotremorine M, but in six experiments, pilocarpine failed to stimulate phosphatidylinositol metabolism significantly (Table 2).

Acetylcholine, carbachol, and oxotremorine M inhibited cAMP formation to an extent indistinguishable from wild-type, whereas pilocarpine inhibited cAMP formation less than wild-type at comparable receptor densities. The EC_{50} value for adenylyl cyclase inhibition was inversely dependent on the receptor density, as was found for wild-type (20), and the slope of this relationship was greater than that for wild-type, which is consistent with the observed 2 orders of magnitude lower affinity of agonists for the receptor (Table 3). The relationship between the EC_{50} for adenylyl cyclase inhibition and the affinity of agonists for the receptor is more complicated than the relationship between EC_{50} for stimulation of phosphatidylinositol metabolism and agonist affinity (20), making a comparison of EC_{50} differences and affinity differences more difficult. The limiting slope and intercept of these plots are interpretable in terms of simple relationships, as was done with wild-type (20); however, the lower agonist affinity observed with the Y403F mutant requires that receptor sites density be greater for the mutant than for wild-type to allow a similar analysis. The experimentally accessible range of receptor concentrations was less than that available for wild-type, and this type of analysis was not possible.

Discussion

Substitution of phenylalanine for the conserved tyrosine in the sixth transmembrane helix seems to meet the general criteria of a nondisruptive deletion (34). The mutation removes a side chain functional group that is involved in a specific interaction and replaces it with a smaller group that does not seem to be involved in overall structural stability. The calculated $\Delta(\Delta G°)$ values of ~0.5 Kcal/mol for antagonists and ~2.5 Kcal/mol for agonists are consistent with the elimination of a hydrogen bond in the ligand bound mutant receptor state that exists in the wild-type receptor (Table 1) (32). An alternative explanation for the role for this tyrosine is as part of an aromatic cation-π binding site for the ligand amine, as was proposed on the basis of molecular modeling (35). Because tyrosine is predicted to be a stronger locus of cation-π binding potential than phenylalanine due to the negative electrostatic potential of the hydroxyl oxygen (36), the distinction between the tyrosine hydroxyl being involved in a hydrogen bond or contributing negative electrostatic potential to a cation-π site cannot be made with the available data. The absence of high resolution structures of the receptor and receptor/ligand complexes necessarily limits any interpretation. A reasonable explanation of these data is that the tyrosine hydroxyl in muscarinic receptors forms a hydrogen bond, of which the strength is important to the binding of the native agonist acetylcholine.

Results presented here and elsewhere (14) confirm the importance of tyrosine residues in the binding of agonists, especially the native agonist acetylcholine and its close analog carbachol, and their relative unimportance in the binding of antagonists. The contrast between the importance of this tyrosine residue in agonist and antagonist binding suggests a role for this residue in the mechanism of receptor activation of G proteins because its absence in m3 muscarinic receptor was coincident with a negative effect on receptor activation. Wess *et al.* (15) proposed such a role for the conserved tyrosine in the sixth transmembrane helix of the m3 muscarinic receptor, whereas results presented here suggest little or no role in receptor activation of G proteins for this residue in the m2 muscarinic receptor.

Site-directed mutagenesis of each of four transmembrane tyrosine residues in the m3 muscarinic receptor resulted in receptors with decreased affinity for acetylcholine and carbachol. The largest decrease in agonist affinity among these tyrosine mutants occurred at residue 506 (58- and 27-fold for

TABLE 3

Effect of Y403F mutation on adenylyl cyclase inhibition in whole-cell assays

EC_{50} values for the inhibition of adenylyl cyclase activity are reported as a range that varies inversely with [R]. Maximal inhibition is reported as mean ± standard deviation except for pilocarpine, for which inhibition was variable and increased with increasing [R] as in wild-type. These values are compared with the wild-type values for the same range of receptor site densities observed in wild-type-expressing CHO cells from data previously reported (20).

Agonist	*n*	EC_{50}	Inhibition	[R]	Wild-type EC_{50}	Wild-type inhibition
		μM	*%*	*pmol · dm*$^{-2}$	*μM*	*%*
Acetylcholine	3	1.7–4.9	71.3 ± 4.9	5.0–17	0.014–0.07	80.0 ± 3.6
Carbachol	6	1.3–37	70.8 ± 5.1	5.0–33	0.036–0.5	65.4 ± 5.1
Oxotremorine M	5	0.6–4.9	74.4 ± 3.7	5.0–23	0.0087–0.28	76.2 ± 2.5
Pilocarpine	4	10–110	19 –43	5.0–23	3.4–15	37–62

acetylcholine and carbachol, respectively), whereas antagonist affinities were reduced only a few-fold (15). We mutated the homologous residue in the m2 muscarinic receptor, Tyr403, and found that antagonist affinities decreased by 2-fold but agonist affinities decreased by ~280- and ~180-fold for acetylcholine and carbachol, respectively. In contrast to the results from the m3 muscarinic receptor functional coupling, the inhibition of adenylyl cyclase did not seem to be affected beyond that expected from the decrease in receptor affinity for acetylcholine and carbachol. Stimulation of phosphatidylinositol metabolism was affected, consistent with the decreased agonist affinity, whereas the maximal response was greater than wild-type at comparable receptor densities.

The scheme in Fig. 4 is an extension of the ternary complex equilibrium binding model (Fig. 1) that takes into account coupling via both the agonist/receptor binary complex and the agonist/receptor/G protein ternary complex (20). The model describes the effect of G protein-coupled receptor activation on the steady state concentration of activated G protein (G') as a function of agonist, receptor, and G protein concentrations; the affinities for each of these for each other; and the rate constants for G protein activation and inactivation. If effector coupling is proportional to activated G protein concentration, then the model describes the effect of G protein-coupled receptor activation on effector coupling. The model predicts a pattern of behavior for the two parameters observable in effector coupling assays, the maximal response, and the concentration of agonist that produces a half-maximal response (EC_{50}). As the receptor density increases, maximal response increases while the EC_{50} is unchanged and equal to the lower affinity agonist dissociation constant, until G protein concentration becomes limiting. When G protein concentration is limiting, further increase in receptor concentration has no effect on maximal response, but the EC_{50} decreases as less agonist is required for a given response. Between the extremes of limiting receptor concentration and limiting G protein concentration, both parameters are predicted to vary with varying receptor density. The placement, breadth, and shape of this transition depend on the receptor/G protein affinity and the ratio of the agonist/receptor/G protein affinity and the agonist/receptor affinity (a parameter referred to as α).

The scheme in Fig. 4 explains the observed effects of variable cell-surface receptor density on effector coupling in m2 muscarinic receptor-expressing CHO cells (20). The EC_{50}

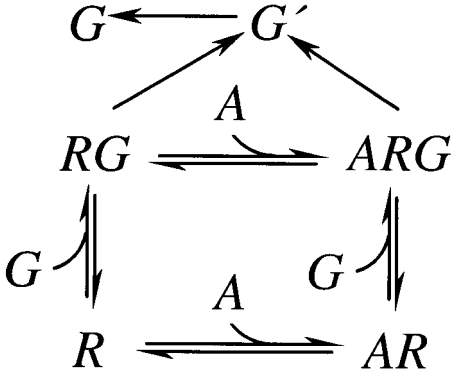

Fig. 4. Ternary complex model with kinetic pathways toward G protein activation and inactivation. G', activated G protein. See legend to Fig. 1 for explanation of receptor states.

value of the inhibition of adenylyl cyclase was found to be inversely proportional to receptor density, whereas the maximal response was constant with varying receptor density for full agonists acetylcholine, carbachol, and oxotremorine M. Pilocarpine displayed the same effect of receptor density on EC_{50}; the maximal effect, however, was reduced relative to the other agonists (partial agonism) at the low end of the receptor density range examined and was indistinguishable from the other agonist effect at the high end of receptor density. In contrast, the EC_{50} value for the stimulation of phosphatidylinositol metabolism was constant and approximately equal to the K_M binding constant for each agonist, with varying receptor density, but the maximal response increased with receptor density. The different pattern of behavior of the two effector coupling systems over the same receptor density range was rationalized as the muscarinic receptor coupling to adenylyl cyclase via a relatively high affinity G protein and coupling to phosphatidylinositol metabolism via a relatively low affinity G protein. The model rationalized the partial agonism observed with pilocarpine and the negative antagonist observed with QNB, NMS, and hyoscyamine in adenylyl cyclase assays.

Results for pilocarpine in the Y403F mutant differ from those for the other agonists in two respects that have interpretable significance on the effects of the Y403F mutation. The α values, a measure of intrinsic efficacy, calculated from data in Table 1 were found to be greater than wild-type for acetylcholine, carbachol, and oxotremorine M but less than wild-type for pilocarpine. The maximal response observed in both physiological assays for pilocarpine was less than that found for wild-type at comparable receptor density, whereas the response found with acetylcholine, carbachol, and oxotremorine M was the same or better than that for wild-type. The α value is related to the ability of an agonist to produce a physiological response because it is a measure of the ability of the agonist to promote the formation of the agonist/receptor/G protein complex at the expense of the agonist/receptor complex. The predicted effect of these changes in α values is that the maximal response in physiological assays would be equal to or greater than that for wild-type for acetylcholine, carbachol, and oxotremorine M and equal to or less than that for wild-type for pilocarpine.

Not included in the scheme in Fig. 4 are possible effects of multiple G proteins, coupling via α and $\beta\gamma$ G protein subunits, or multiple active conformational states that are differentially stabilized by agonist. In addition, differences between the wild-type and Y403F clonal cell lines in G protein concentration or in the ratio of multiple G proteins or mutational alterations in the composite rate constant for G protein activation would be expected to affect the maximal response. The effect of a change in α value on maximal response is predicted to be sensitive to differences in the affinity of the receptor for G protein such that an effect visible in one assay may not be visible in another if it were coupled via a different G protein. The same effect can be explained by activation of a single G protein via α and $\beta\gamma$ G protein subunits. This would require expansion of the model in Fig. 4 at the composite activation steps to include separate activation routes and different subunit/effector concentration dependencies.

The change in single G protein concentration or ratio of G proteins that act similarly or in the composite rate constant for G protein activation cannot account for our results be-

cause they would affect the maximal response to a similar extent for all agonists and would affect the inhibition of cAMP formation and stimulation of phosphatidylinositol metabolism similarly. Results from a reconstituted system of purified m2 muscarinic receptor and G_i indicated that pilocarpine and carbachol promoted GTPase activity similarly (37), suggesting that if multiple active conformations that specifically activate G protein agonist exist, they are not significant in wild-type; however, this may not be true for the Y403F mutant. The cell lines used for these studies contain a mixture of G_{i2} and G_{i3}; G_{i1} and G_o are not present,[1] which limits the potential for changes in G protein ratio having a differential effect on the wild-type and mutant-expressing cell lines. Differential effects of $\beta\gamma$ subunit stimulation of phospholipase C seem unlikely in two respects. This effect would require agonist-specific stimulation of G proteins in the mutant that is not observed in wild-type. If this occurred in our experiments, then the differential mixture of $\beta\gamma$ subunits that might result would have to have a differential effect on phospholipase Cβ isozymes. Recent results with phospholipase Cβ3 indicate that there is little difference in the potencies among different $\beta\gamma$ subunits, apart from the very low activity of $\beta1\gamma1$ (38). Although there are many factors, some of which are difficult to control for, that have the potential to complicate the interpretation of the results, the simplest explanation is that the observed agonist-specific change in α value between wild-type and the mutant receptor is the best explanation of the agonist-specific changes observed in functional assays.

The Y403F mutation in m2 muscarinic receptor seems to have affected only the ligand binding affinities of the receptor. Our data are consistent with this tyrosine hydroxyl being involved in a hydrogen bond that is important in the stability of the agonist bound state. This tyrosine also seems to be more important in the free receptor than in the G protein-associated receptor state for acetylcholine, carbachol, and oxotremorine M. Effects observed in physiological assays can be explained by reductions in the absolute receptor/agonist affinity and the relative affinity of agonists for the free receptor and the receptor/G protein complex.

These results help explain an otherwise difficult to rationalize result from mutagenesis experiments on the proline residue in the sixth transmembrane domain of the m3 muscarinic receptor. This proline is one residue away from the tyrosine and is conserved in virtually all G protein-coupled receptors (the major exception is the olfactory receptors). If the tyrosine is part of a binding and trigger mechanism for G protein activation, as was suggested (15), then it seems reasonable to expect that the adjacent proline, with its conformational flexibility, also is an integral part of the trigger. Support for this model can be found in the results of molecular dynamics simulations on the transmembrane segments of 5-hydroxytryptamine receptor that suggested agonist but not antagonist binding would result in large movements in the transmembrane helices 5 and 6 (39). A trigger mechanism of receptor activation suggests that the agonist/receptor/G protein complex can assume an active and inactive conformation. However, mutation of this proline residue in the m3 muscarinic receptor had no effect on antagonist binding, little effect on agonist binding, and no effect on its ability to stimulate phosphatidylinositol metabolism (40). In the Y403F m2 muscarinic receptor, agonist binding to the higher affinity G protein-coupled receptor state was sensitive to guanine nucleotides, and the mutant receptor was capable of eliciting a functional response similar to that of wild-type, whereas in the Y506F m3 muscarinic receptor (15), agonist binding was not sensitive to guanine nucleotides, and the mutant receptor was less capable than wild-type of eliciting a functional response. This lack of sensitivity to guanine nucleotides in the m3 subtype mutant suggests a relative decrease in α values for acetylcholine and carbachol, for which values increase in the m2 subtype. An explanation of the results from the m3 muscarinic receptor is that, as in the m2 muscarinic receptor, the conserved tyrosine residue is primarily involved in an interaction that stabilizes the agonist bound state. This reduced ability to stimulate phosphatidylinositol metabolism has the same mechanistic origin as a similar effect seen only with pilocarpine in the m2 subtype. There is no reason to believe that a single mutation could not have multiple effects, but the data suggest that these mutations in or near the putative agonist binding site affect only binding. The trigger mechanism, if it exists at all, lies elsewhere, perhaps involving the seventh transmembrane helix, because the proline in that helix had the most dramatic effect on coupling in the m3 subtype (40).

Acknowledgments

We thank D. J. Broderick and G. L. Peterson for assistance with the experiments.

References

1. Kubo, T., K. Fukuda, A. Mikami, A. Maeda, H. Takahashi, M. Mishina, T. Haga, K. Haga, A. Ichiymama, K. Kangawa, M. Kojima, H. Matsuo, T. Hirose, and S. Numa. Cloning, sequencing and expression of complementary DNA encoding the muscarinic acetylcholine receptor. *Nature (Lond.)* **323:**411–416 (1986).
2. Peralta, E. G., J. W. Winslow, G. L. Peterson, D. H. Smith, A. Ashkenazi, J. Ramachandran, M. I. Schimerlik, and D. J. Capon. Primary structure and biochemical properties of an M_2 muscarinic receptor. *Science (Washington D. C.)* **236:**600–605 (1987).
3. Peralta, E. G., A. Ashkenazi, J. W. Winslow, D. H. Smith, J. Ramachandran, and D. J. Capon. Distinct primary structures, ligand-binding properties and tissue-specific expression of four human muscarinic acetylcholine receptors. *EMBO J.* **6:**3923–3929 (1987).
4. Bonner, T. I., N. J. Buckley, A. C. Young, and M. R. Brann. Identification of a family of muscarinic acetylcholine receptor genes. *Science (Washington D. C.)* **237:**527–532 (1987).
5. Bonner, T. I., A. C. Young, M. R. Brann, and N. J. Buckley. Cloning and expression of the human and rat m5 muscarinic acetylcholine receptor genes. *Neuron* **1:**403–410 (1988).
6. Nathanson, N. M. Molecular properties of the muscarinic acetylcholine receptor. *Annu. Rev. Neurosci.* **10:**195–236 (1987).
7. Hille, B. *Ionic Channels of Excitable Membranes*. Sinauer, Sunderland, MA (1992).
8. Nakayama, T. A., and H. G. Khorana. Orientation of retinal in bovine rhodopsin determined by cross-linking using a photoactivatable analog of 11-*cis*-retinal. *J. Biol. Chem.* **265:**15762–15769 (1990).
9. Strader, C. D., I. S. Sigal, M. R. Candelore, E. Rands, W. S. Hill, and R. A. F. Dixon. Conserved aspartic acid residues 79 and 113 of the β-adrenergic receptor have different roles in receptor function. *J. Biol. Chem.* **263:**10267–10271 (1988).
10. Fraser, C. M., S. Arakawa, W. R. McCombie, and J. C. Venter. Cloning, sequence analysis, and permanent expression of α_2-adrenergic receptor in Chinese hamster ovary cells. *J. Biol. Chem.* **264:**11754–11761 (1989).
11. Page, K. M., C. A. M. Curtis, P. G. Jones, and E. C. Hulme. The functional role of the binding site aspartate in muscarinic acetylcholine receptors, probed by site-directed mutagenesis. *Eur. J. Pharmacol.* **289:**429–437 (1995).
12. Dixon, R. A. F., I. S. Sigal, and C. D. Strader. Structure-function analysis of the β-adrenergic receptor. *Cold Spring Harbor Symp. Quant. Biol.* **53:**487–497 (1988).
13. Nardone, J., and P. G. Hogan. Delineation of a region in the B2 bradykinin

[1] J. Robishaw, unpublished observations.

receptor that is essential for high-affinity agonist binding. *Proc. Natl. Acad. Sci. USA* **91:**4417–4421 (1994).
14. Wess, J., D. Gdula, and M. R. Brann. Site-directed mutagenesis of the m3 muscarinic receptor: identification of a series of threonine and tyrosine residues involved in agonist but not antagonist binding. *EMBO J.* **10:** 3729–3734 (1991).
15. Wess, J., R. Maggio, J. R. Palmer, and Z. Vogel. Role of conserved threonine and tyrosine residues in acetylcholine binding and muscarinic receptor activation: a study with m3 muscarinic receptor point mutants. *J. Biol. Chem.* **267:**19313–19319 (1992).
16. Nakayama, T. A., and H. G. Khorana. Mapping of the amino acids in membrane-embedded helices that interact with the retinal chromophore in bovine rhodopsin. *J. Biol. Chem.* **266:**4269–4275 (1991).
17. Huang, R.-R. C., P. P. Vicario, C. D. Strader, and T. M. Fong. Identification of residues involved in ligand binding to the neurokinin-2 receptor. *Biochemistry* **34:**10048–10055 (1995).
18. De Lean, A., J. M. Stadel, and R. J. Lefkowitz. A ternary complex model explains the agonist-specific binding properties of the adenylate cyclase coupled β-adrenergic receptor. *J. Biol. Chem.* **255:**7108–7117 (1980).
19. Costa, T., Y. Ogino, P. J. Munson, O. Onaran, and D. Rodbard. Drug efficacy at guanine nucleotide-binding regulatory protein-linked receptors: thermodynamic interpretation of negative antagonism and of receptor activity in the absence of ligand. *Mol. Pharmacol.* **41:**549–560 (1992).
20. Vogel, W. K., V. A. Mosser, D. A. Bulseco, and M. I. Schimerlik. Porcine m2 muscarinic acetylcholine receptor-effector coupling in Chinese hamster ovary cells. *J. Biol. Chem.* **270:**15485–15493 (1995).
21. Samama, P., S. Cotecchia, T. Costa, and R. J. Lefkowitz. A mutation-induced activated state of the β_2-adrenergic receptor: extending the ternary complex model. *J. Biol. Chem.* **268:**4625–4636 (1993).
22. Samama, P., G. Pei, T. Costa, S. Cotecchia, and R. J. Lefkowitz. Negative antagonists promote an inactive conformation of the β_2-adrenergic receptor. *Mol. Pharmacol.* **45:**390–394 (1994).
23. Chidiac, P., T. E. Herbert, M. Valiquette, M. Dennis, and M. Bouvier. Inverse agonist activity of β-adrenergic antagonists. *Mol. Pharmacol.* **45:** 490–499 (1994).
24. Birdsall, N. J. M., A. S. V. Burgen, and E. C. Hulme. The binding of agonists to brain muscarinic receptors. *Mol. Pharmacol.* **14:**723–736 (1978).
25. Peterson, G. L., and M. I. Schimerlik. Large scale preparation and characterization of membranes-bound and detergent-solubulized muscarinic acetylcholine receptor from pig atria. *Prep. Biochem.* **14:**33–74 (1984).
26. Peterson, G. L., A. Toumadje, W. C. Johnson, Jr., and M. I. Schimerlik. Purification of recombinant porcine m2 muscarinic acetylcholine receptor from Chinese hamster ovary cells: circular dichroism spectra and ligand binding properties. *J. Biol. Chem.* **270:**17808–17814 (1995).
27. Vandeyar, M. A., M. P. Weiner, C. J. Hutton, and C. A. Batt. A simple and rapid method for the selection of oligodeoxynucleotide-directed mutants. *Gene* **65:**129–133 (1988).
28. Sanger, F., S. Nicklen, and A. R. Coulson. DNA sequencing with chain-terminating inhibitors. *Proc. Natl. Acad. Sci. USA* **74:**5463–5467 (1977).
29. Lee, W., K. J. Nicklaus, D. R. Manning, and B. B. Wolfe. Ontogeny of cortical muscarinic receptor subtypes and muscarinic receptor-mediated responses in rat. *J. Pharmacol. Exp. Ther.* **252:**482–490 (1990).
30. Salomon, Y. Adenylate cyclase assay, in *Advances in Cyclic Nucleotide Research*. Raven Press, New York, 35–55 (1979).
31. Marquardt, D. W. An algorithm for least-squares estimation of nonlinear parameters. *J. Soc. Ind. Appl. Math.* **11:**431–441 (1963).
32. Fersht, A. R. Relationships between apparent binding energies measured in site-directed mutagenesis experiments and energetics of binding and catalysis. *Biochemistry* **27:**1577–1580 (1988).
33. Scatchard, G. The attractions of proteins for small molecules and ions. *Ann. N. Y. Acad. Sci.* **51:**600–672 (1949).
34. Fersht, A. R., R. J. Leatherbarrow, and T. N. C. Wells. Structure–activity relationships in engineered proteins: analysis of use of binding energy by linear free energy relationships. *Biochemistry* **26:**6030–6038 (1987).
35. Trumpp-Kallmeyer, S., J. Hoflack, A. Bruinvels, and M. Hibert. Modeling of G-protein-coupled receptors: application to dopamine, adrenaline, serotonin, acetylcholine, and mammalian opsin receptors. *J. Med. Chem.* **35:** 3448–3462 (1992).
36. Dougherty, D. A. Cation-π interactions in chemistry and biology: a new view of benzene, Phe, Tyr, and Trp. *Science (Washington D. C.)* **271:**163–168 (1996).
37. Tota, M. R., and M. I. Schimerlik. Partial agonist effects on the interaction between the atrial muscarinic receptor and the inhibitory guanine nucleotide-binding protein in a reconstituted system. *Mol. Pharmacol.* **37:**996–1004 (1990).
38. Exton, J. H. Cell signalling through guanine-nucleotide-binding regulatory proteins (G proteins) and phospholipases. *Eur. J. Biochem.* **243:**10–20 (1997).
39. Zhang, D., and H. Weinstein. Signal transduction by a 5-HT_2 receptor: a mechanistic hypothesis from molecular dynamics simulations of the three-dimensional model of the receptor complexed to ligands. *J. Med. Chem.* **36:**934–938 (1993).
40. Wess, J., S. Nanavati, Z. Vogel, and R. Maggio. Functional role of proline and tryptophan residues highly conserved among G protein-coupled receptors studied by mutational analysis of the m3 muscarinic receptor. *EMBO J.* **12:**331–338 (1993).

Send reprint requests to: Dr. Michael I. Schimerlik, Department of Biochemistry and Biophysics, 2011 ALS, Oregon State University, Corvallis, OR 97331-7305. E-mail: schimerm@ucs.orst.edu